Proceeding of the IEEE
International Conference on Robotics and Biomimetics
Dali, China, December 2019

Wing Sail Land-yacht Modeling And System Verification*

Yibing Dong[1], Xiao Ding[1], Zhijun Li[1], Lianxin Zhang[1],
Hengli Liu[1,3], Ning Ding[2], Zhenglong Sun[1,2], Huihuan Qian[1,2,†]

***Abstract*— Wind-driven vehicle is a kind of promising way to utilize wind energy due to its non-pollution feature. This paper presents a practical design of the wind-driven vehicle in the form of land-yacht, which is equipped with a wing sail and a micro-controller unit. Theoretical analysis and simulation were performed to find the total force coefficient corresponding to each combination of attack angle and heading angle, and the best attack angle corresponding to each different heading angle. A prototype was built and tested in a wind-field environment. The simulation and experiment were concordant, both of which showed the relation between the movement of land-yacht and these angles when moving upwind well.**

***Index Terms*— Wind-driven, Land-yacht, Wing Sail, Moving Upwind.**

Fig. 1. Rendering of wing sail land-yacht traveling on the road.

I. Introduction

In the 21st century, air pollution is one of the most severe common problems in the world, and motor vehicle exhaust is the primary source of air pollution in many regions. Research showed that about half of all deaths caused by air pollution were attributed to vehicle exhaust [1]. Most vehicles generate kinetic energy by burning gasoline. During the process of combustion of gasoline, monoxide, nitrogen oxides, and particulates with diameter less than 2.5μm (PM 2.5), which are the primary components of air pollution, are released [2][3].

Therefore, there is an urgent need to prevent air pollution from becoming more serious, and the energy supply of some vehicles should be changed. Electric energy and wind energy are the clean energy source commonly used for transportation. Although electric energy has the advantage of convenient storage and continuous stability, the process of generating electricity still creates pollution. Atmospheric emissions, such as sulfur dioxide and PM2.5, from coal-fired power plants, pose a significant burden on human health [4].

By contrast, as a kind of energy that caused by differential heating level of the earth's surface, wind power is more environmentally friendly. Wind power is always being supplemented by the sun. Hence it is entirely renewable, free of polluting, and also economical [5]. These features give wind energy the potential to become one of the new energy resources that will replace the traditional fuels used in transportation. Since a long time ago, sailboats have been used as the main transportation in a waterway. By adjusting the angle of the sails and rudders, the sailboat can move upwind, tack upwind, and even faster than wind. However, because of the more complicated road conditions on the land, the wind energy has not yet been used widely on land-yachts. Being inspired by sailboat, this paper proposes a kind of wing sail land-yacht which is powered by wind energy. It is safer and easier to steer than sailboats taking into consideration that the direction is controlled by wheels.

Cloth sails have been used in attempts of developing wind-driven land-yachts. However, the cloth sails are not stable and are prone to deform, and have a wide no-go zone. When the heading angle (the angle between the heading direction of the land-yacht and wind direction) is in it, the land-yacht will lose the forward propulsion that applied on the sail [6]. Compared with cloth sails, wing sails have advantages of robustness, convenience of adjusting the angle, and little no-go zone which is because of the wide-angle range of the resultant force applied on the wing sail.

Previously, the researches on wing sail land-yachts were mainly about the utilization of them in the exploration of Antarctic or other harsh environment [7][8]. But the mentioned advantages such as robustness and little no-go zone, together with the property of land-yacht whose heading direction could be convenient to adjust, make it significantly valuable for develop the utilization of wing sail land-yachts in general terrestrial environment. The movement of the wing sail land-yacht in downwind conditions has been researched before [9][10][11]. And some specific parameters that may affect the movement have also been researched [8][11][12][13]. In this paper, the simulation and experiment will focus on the upwind movement of the wing sail land-

*This work is supported by Project U1613226 and U1813217 supported by NSFC, China, Project 2019-INT009 from the Shenzhen Institute of Artificial Intelligence and Robotics for Society, the Shenzhen Science and Technology Innovation Commission, fundamental research grant KQJSCX20180330165912672, R&D Project of Ministry of housing and urban construction (Grant No.2018-K8-034).

[1]The Chinese University of Hong Kong, Shenzhen, China. Yibing Dong, Xiao Ding, and Zhijun Li contributed to this work equally.
[2]Shenzhen Institute of Artificial Intelligence and Robotics for Society.
[3]University of Science and Technology of China.
[†]Corresponding author: hhqian@cuhk.edu.cn

yacht.

One of the main concerns of wind energy is its unstable speed and direction. Therefore, in order to use wind energy to drive the land-yachts by wing sails, it is an important issue to control the wing sail land-yacht to travel upwind. The best attack angles under different situations of heading angles should be found, and the land-yacht should have the ability to change the direction of the wing sail according to the wind direction detected by the sensors to maintain its speed and acceleration.

In this paper, a new design of wing sail land-yacht is introduced, and the rendering of it is in Fig.1. The structure of the vehicle, the wing sail, and the circuit are included. The overall design parameters that concerned are illustrated in Section II. To find the theoretical best attack angle under each different heading angle, wing sail was modeled, and the stress condition of it was simulated in section III. After the experiment, the practical best attack angles corresponding to different heading angles when the land-yacht moving upwind were found and compared with the simulated result. The variation tendency of the acceleration was also compared with the simulated variation tendency of the total coefficient, which is proportional to the acceleration. The experiment result is in concord with the simulated result.

II. System Design

A. Land-yacht Body

The wing sail land-yacht mainly contains two parts: the land-yacht body and the wing sail. The body of the land-yacht is a four-wheeled steel frame that ensures the stability of the land-yacht during driving, as shown in Fig. 2.

In order to make the land-yacht body lighter, the connecting parts absorbing less force are made of plastic material. The front wheel of the land-yacht is a steering wheel, and the rear wheel is a non-power wheel. The wheels of the land-yacht are solid rubber slicks. A servo motor that controls the mechanical steering structure is set on the front of the vehicle body, and the steering angle is from minus 60 degrees to 60 degrees. A wind sensor is set above the front of the land-yacht body, while the battery and the Raspberry Pi control panel are mounted on the bottom center of an acrylic plate fixed on the land-yacht body, and the wing sail is mounted above the center of plate.

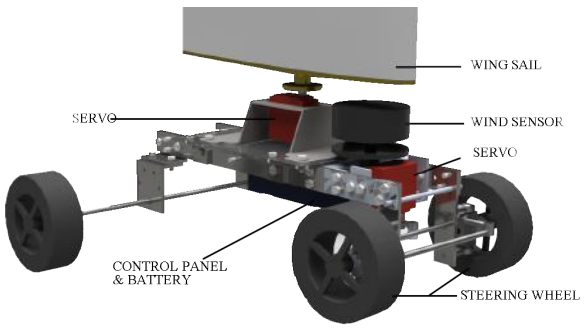

Fig. 2. The physical structure of the land-yacht body.

B. Controlling System

The electric system is the core of the wing sail land-yacht system that collects meaningful data and implements the auto-control process. According to the purpose, the integrated system can be divided into three parts, the power supply system, data collection and transmission system, and the dynamical system. The power supply system is a set of batteries with a transformer module, which ensures that the voltage is stable within the range that can maintain the system working. The data collection and transmission system contain a wind sensor (CALYPSO), an Inertial measurement unit (HI219), and a Wi-Fi unit. The wind sensor that measures the wind direction, together with the IMU, which is aimed at determining the heading angle, collect data to help adjust the heading and the attack angle of the wind sail land-yacht. These data operated by the microprocessor will be transported to computers via integrated Wi-Fi unit. The Dynamical system consists of mechanical structures and two servo motors. The first servo motor (180 degrees) controls the front-wheel steering which determines the heading, and the second servo motor (270 degrees) controls the attack angle.

C. Wing Sail

Given the maturity of relevant technology, the wing sails among NACA series were considered. Cylinder sails are used for a more straightforward simulation than the sails which are uneven on height, because in this situation, the model could be regarded as a 2D model. As a result, NACA 0015 was finally chosen.

The function of the curve of boundary of the section of a wing sail should be (for $y_t \geq 0$) [9]:

$$y_t = \frac{T}{0.2}(a_0\sqrt{x} + a_1 x + a_2 x^2 + a_3 x^3 + a_4 x^4) \quad (1)$$

Where for NACA 0015, $a_0 = 0.2969$, $a_1 = -0.126$, $a_2 = -0.3516$, $a_3 = 0.2843$, and $a_4 = -0.1036$, and the

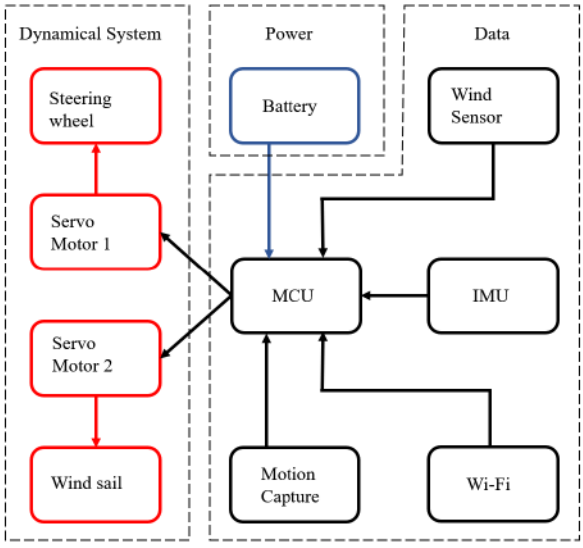

Fig. 3. Power and data flow of the wing sail land-yacht

symmetry axis of the boundary is the x-axis. The required thicknesses of a wing sail can be achieved by adjusting the value of T. In this research, 0.15 is chosen as the value.

The wing sail is fixed to the base by four screws. The base is connected to the servo motor via a flange. The rotating shaft of the wing sail passes through the center of the land-yacht so that the land-yacht body is balanced when wing sail is stressed.

III. Wing Sail Modeling and Simulation

A. Assumption

The modeling and simulation of the wing sail are based on the following assumptions:

1) : The fluid around is ideal gas (ideal air) to ensure more attention is paid to the major object: the control of the wing sail land-yacht.

2) : The uniqueness and certainty of the heading angle mean that among this research, the variety of the wind direction and strength in the range of the space around the sail are ignored.

3) : During the simulation, the effects of wind which are on the land-yacht body, such as the resistance and the friction, are not considered.

B. Modeling Analysis

For a particular wing sail, as shown in Fig. 4 and Fig. 5, there exists a set of parameters that influence the performance of the wing sail.

The parameters include the attack angle (α), which represents the angle between the wind direction and the spindle of the wing sail, the heading angle (γ), and the coefficient of lift (C_L) and drag (C_D). C_L and C_D are the coefficients which are with respect to the shape of the wing sail and the nature of surrounding fluid [14]. They are used to calculate the lift force (L) and drag force (D) applied on the wing

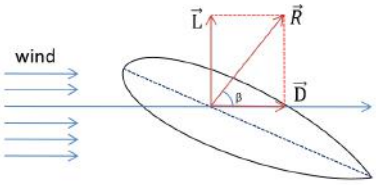

Fig. 4. The relationship among the drag force D, the lift force L and the resultant force R.

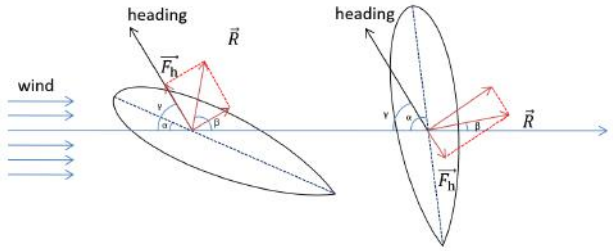

Fig. 5. Left: A demonstration of applied force the effective component F_h. Right: The instant of failure to drive the cart.

sail, which are the components of the force applied on wing sail by wind that are perpendicular and parallel to the wind respectively. C_L and C_D are defined by:

$$C_L = \frac{L}{\frac{1}{2}\rho V_\infty^2 S} \tag{2}$$

$$C_D = \frac{D}{\frac{1}{2}\rho V_\infty^2 S} \tag{3}$$

where ρ is the density of the medium, V_∞ is average wind speed, and S is the area of the wing sail.

NACA 0015 is, as stipulated, a symmetrical and streamlined body. As shown in Fig.4, after the wind applying on the wing sail, a lift force and a drag force emerge. The vector sum of these two component forces is denoted by R. Combining with the requirement to power the land-yacht towards an arbitrary direction, the component of R onto the determined direction becomes the decisive parameter.

C_L and C_D are important factors to derive R. Therefore, the coefficient C is involved.

$$C^2 = C_L^2 + C_D^2 \tag{4}$$

$$R = \frac{1}{2} C \rho V_\infty^2 S \tag{5}$$

The force along the heading direction is:

$$F_h = R\cos(180^\circ - \gamma - \beta) \tag{6}$$

Correspondingly, a total force coefficient C_h, which is proportional to F_h and will be attained by simulation, is defined by:

$$C_h = \frac{F_h}{\frac{1}{2}\rho V_\infty^2 S} \tag{7}$$

Where $\beta = \arctan(C_L/C_D)$ is the deflection angle and γ is the heading angle. In principle, larger F_h is wanted. In the analysis part, these coefficients are involved.

When the attack angle is low, C_L is usually much larger than the C_D under an ideal situation. This means the deflection angle between the wind velocity and resultant force directions is a little less than 90 degrees. If the attack angle increases, this deflection angle tends to decrease.

Therfore, as shown in the Fig.5, there exists a range of heading angle in which the wind could not power the land-yacht. It is because there are not any positive component forces along the heading direction whatever the attack angle is. Therefore, the performance of the wing sail should be necessarily simulated to estimate this no-go zone. Furthermore, proper attack angle should be chosen to maximize F_h.

An 80 cm high cylinder NACA 0015 sail with a 30 cm long spindle was analyzed on account of the size of the land-yacht.

C. Simulation

C_L and C_D are simulated by an ANSYS program, and the Fluent module was involved. The coefficients of drag and lift force were accessible under circumstances of different attack angles. The Fig.6 shows the result of the simulation.

As expected, when the attack angle is low, the lift function

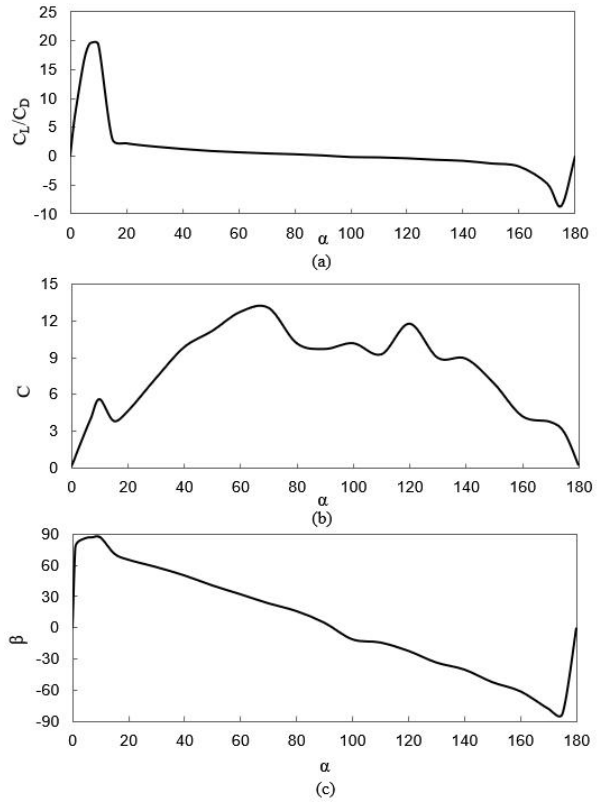

Fig. 6. (a) The curve of the ratio of the coefficient of lift force to drag force vs the attack angle. (b) The curve of the total force coefficient vs the attack angle. (c) The curve of the deflection angle vs the attack angle.

of this wing sail turns to be exercised. The lift force nearly achieves the summit when attack angle is around 10 degrees, while the drag force is relatively small. After 15 degrees, the lift force inclines to decrease, while the drag force gradually becomes dominant.

When the attack angle is less than 10 degrees, the total available force is approximately proportional to it. When the attack angle becomes larger, the force gets larger apparently, but the dominant component turns to be the drag force. It is reasonable for a land-yacht to be moved by dragging forces. As a result, the region with the most massive C is not the most crucial focusing point.

The deflection angle, significantly, shows a linear relationship with attack angle in the interval of high attack angle. It also shows that the resultant force is always nearly perpendicular to the wind velocity when the attack angle is low.

When the heading angle varies, the best attack angle, which makes the component force onto the heading direction of the land-yacht become as large as possible, varies along with it.

Fig. 7 shows that when the heading angle is between 90 degrees and 180 degrees, the land-yacht is moving downwind and the total force coefficients at the best attack angles are large. The resultant forces applied on the wing sail are obviously large enough to drive the land-yacht. Therefore, in Fig. 8, only the best attack angles corresponding to the

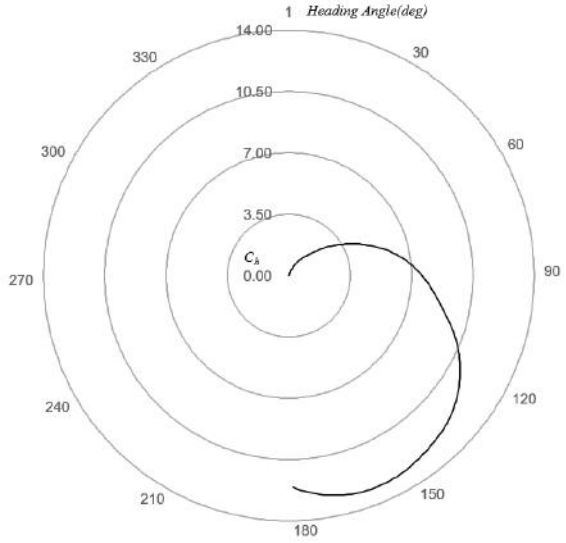

Fig. 7. The maximal total force coefficient (the numbers inside the circle) under the circumstances with different heading angle (degrees around the circumference in the graph) and the corresponding best attack angle.

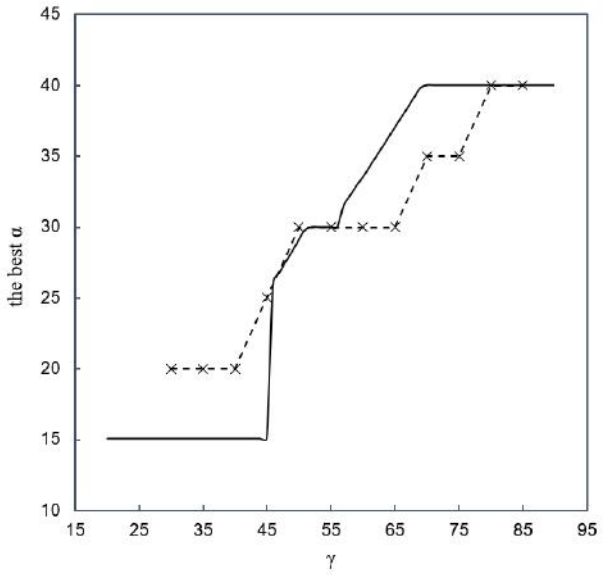

Fig. 8. Curves of the best attack angle over the heading angle.The result of simulation is indicated by a solid line and the result of experiment is indicated by a dashed line. A similar tendency exists in these curves.

heading angles between 0 to 90 degrees were shown and compared with the experiment result. This meant the upwind condition. Fig. 8 shows that the variation tendency of the best attack angle has a ladder-shaped feature.

The simulation showed that the no-go zone is -3 degrees to 3 degrees. When the heading angle is in this range, there is no possibility to drive the land-yacht by wind for no positive components exists on the heading direction. But as Fig. 7 showed, when the heading angle is small, the corresponding maximal total force coefficient is also limited. This means that the practical no-go zone is supposed to be much larger to overcome the inevitable resistance.

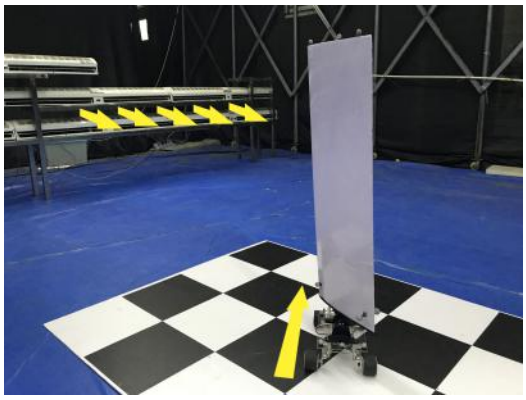

Fig. 9. The experiment environment with the direction of the wind and the heading of land-yacht.

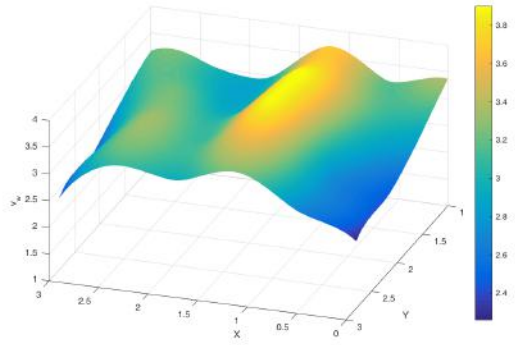

Fig. 10. The wind field in which the experiment was conducted.

IV. Experiment and Analysis

The speed of the land-yacht is expected to be relatively low compared with the wind speed. Therefore, the absolute wind velocity could be approximately considered as the relative wind velocity V_∞. The dynamics equation for the yacht is:

$$Ma = F_h - f \tag{8}$$

Where M is the total mass, a is the acceleration of the land-yacht, and f is the total resistance, which contains rolling friction, air force onto the cart body and inner friction, etc. In the experiment, these resistances were considered to be low enough to be ignored.

A. Wind Field

The real experiment environment is shown in Fig. 9, and the wind field in it was tested and was charted in Fig. 10. The wind was produced by nine identical blowers. Twenty four wind sensors were placed in a 2-meter by 3-meter area, in which the land-yacht moved during the experiment. The area is 1 meter far from the blowers. Every sensor collected the speed of the wind every 10 seconds and collected ten times in total, and the average speed was calculated. The average wind speed was regarded as the wind speed at the position of the wind sensor.

B. Prototype and Verification Experiment

The manufacturing of the prototype has been completed, as shown in Fig. 9. The vehicle part of the prototype is 35 cm long, 20 cm wide and 10 cm high. The front wheelbase is 18 cm, and the rear wheelbase is 25 cm, ensuring that the land-yacht does not roll over during steering. The wing sail is 80 cm high and 30 cm wide (the camber was 30 cm long) and is made of Styrofoam with a smooth plastic film on the outside.

The experiment, which is mainly about the performance of the land-yacht when moving upwind, was conducted to verify the result of the simulation. In the experiment, with each given heading angle and attack angle, the acceleration of the land-yacht was recorded. Both of the heading angle and the attack angle change by 5 degrees every time.

As the theory shows, when the land-yacht is heading upwind, it can move upwind only if the wing attack angle is between the heading angle and the wind direction. The preliminary experiment also showed that the least heading angle and attack angle that could move the land-yacht were 30 degrees and 15 degrees. Therefore, the motions were recorded when the heading angle γ and attack angle α conform: $30\,\mathrm{deg} \leq \gamma \leq 90\,\mathrm{deg}$, $15\,\mathrm{deg} \leq \alpha \leq (\gamma - 10\,\mathrm{deg})$.

The motion path of the land-yacht was recorded by motion capture. Moreover, the wing sail was controlled by Raspberry Pi, which is a micro-controller unit. The Raspberry Pi was used to adjust the heading angle and the attack angle, according to the real-time received wind direction data. It was programmed to ensure the attack angle and heading angle unchangeable. Therefore, the stability of the experiment was enhanced.

The graphs of theoretical total force coefficient and practical average accelerations of the land-yacht according to different heading angles and attack angle are given in Fig. 11. The two independent variables of the graphs are the same, and the dependent variables of them are the total force coefficient and the average acceleration, relatively. Ignoring the air resistance applied on the land-yacht body and the friction, the total force coefficient is proved to be proportional to the total force, F_h, applied on the whole land-yacht, and also proportional to the acceleration. Approximately, the experimental results are basically consistent with the simulation results as both of them show similar variation tendencies.

In some cases of the experiment, the speed of the land-yacht may be enough to influence the magnitude and direction of relative wind power applied on the wing sail. This difference made a fine distinction between the practical and theoretical best attack angles corresponding to heading angles. Firstly, this difference between the absolute and relative wind direction made that the practical best attack angle a little different than the theoretical one. Secondly, when the land-yacht was driven by the wind, the acceleration also changed a little because of the variation of the magnitude of relative wind velocity. And the magnitudes of accelerations which were used to get the practical best attack angles

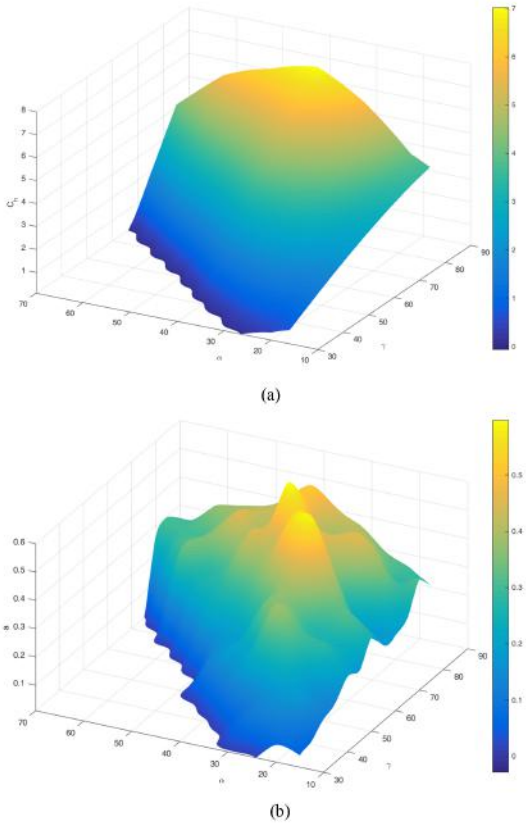

Fig. 11. (a)The theoretical total force coefficient versus attack angle and sail angle. (b)The practical acceleration versus attack angle and sail angle.

corresponding to the heading angle were average values. This also may change the best attack angles. Therefore, it was important to compare the theoretical and practical variation tendencies of the best attack angles. Fig.8 showed that the tendencies are similar, and it also means that the simulation and experiment were reasonable.

V. Conclusion and Future Work

This paper proposes a design of the wind-driven land-yacht. The land-yacht was equipped with a micro-controller unit, which can control the heading direction of the land-yacht and the direction of the wing sail. In order to get the real-time wind velocity, it is also installed with a wind sensor. The wing sail of the land-yacht was modeled and simulated to get the best attack angle corresponding to each heading angle.

The experiment was conducted to verify the realistic acceleration of the land-yacht with every possible combination of attack angle and heading angle. The experimental results are basically consistent with the simulated results.

In the future, numerous additional functions of the wing sail land-yacht can be realized by the micro-controller unit. For example, the wing sail land-yacht can read the environment data and data about its own motion, and use the data to adjust itself real-time to finish the given route and avoid the obstacles.

References

[1] N. Knzli, R. Kaiser, S. Medina, M. Studnicka, O. Chanel, P. Filliger, M. Herry, F. Horak, V. Puybonnieux-Texier, P. Qunel, J. Schneider, R. Seethaler, J.-C. Vergnaud, and H. Sommer, "Public-health impact of outdoor and traffic-related air pollution: a European assessment," *The Lancet*, vol. 356, no. 9232, pp. 795-801, 2000.

[2] R. Goel and S. K. Guttikunda, "Role of urban growth, technology, and judicial interventions on vehicle exhaust emissions in Delhi for 1991-2014 and 2014-2030 periods," *Environmental Development*, vol. 14, pp. 6-21, 2015.

[3] J. Gao, X. Peng, G. Chen, J. Xu, G.-L. Shi, Y.-C. Zhang, and Y.-C. Feng, "Insights into the chemical characterization and sources of PM2.5 in Beijing at a 1-h time resolution," *Science of The Total Environment*, vol. 542, pp. 162-171, 2016.

[4] S. K. Guttikunda and P. Jawahar, "Atmospheric emissions and pollution from the coal-fired thermal power plants in India," *Atmospheric Environment*, vol. 92, pp. 449-460, 2014.

[5] G.M.J. Herbert, S. Iniyan, E.Sreevalsan, and S. Rajapandian, "A review of wind energy technologies", *Renewable and Sustainable Energy Reviews*, vol.11, no.6, pp.1117-1145, 2007.

[6] J. Jouffroy, "A control strategy for steering an autonomous surface sailing vehicle in atacking maneuver" in *Proc. IEEE Int. Conf. on Systems, Man, and Cybernetics*, San Antonio, USA, 2009.

[7] J. Chen, S. Xie, J. Luo, and H. Li, "Wind-driven land-yacht robot mathematical modeling and verification," *Industrial Robot: An International Journal*, vol. 43, no. 1, pp. 77-90, 2016.

[8] S. Xie, J. Chen, H. Li, J. Luo, H. Pu, and Y. Peng, "The research on wing sail of a land-yacht robot," *Advances in Mechanical Engineering*, vol. 7, no. 12, p. 168781401562314, 2015.

[9] S. Xie, K. Feng, Y. Peng, J. Luo, J. Chen, and J. Gu, "Design and analysis of an autonomous controlled four wheeled land yacht" in *Proc. IEEE Int. Conf. on Information and Automation*, Hailar, China, 2014.

[10] H. Amini, M. Rad, and A. Fakhraee, "Comparison Final Velosity Between Sailing Boat With a Rigid Airfoil and Cloth Sail," *Fluids Engineering*, 2006.

[11] J. Chen, S. Xie, H. Li, J. Luo, and C. Zhao, "Roughness effect on airfoil aerodynamic performance for land-yacht robot," *Journal of Renewable and Sustainable Energy*, vol. 8, no. 2, p. 025701,2016.

[12] J. Chen and H. Li, "Airfoil Optimization of Land-Yacht Robot Based on Hybrid PSO and GA," *International Journal of Pattern Recognition and Artificial Intelligence*, p. 1959041, Nov. 2019.

[13] J. Moore, "Measuring the Speed of a Model Land Yacht with Varying Sail Shape and Wind Power," 01-Jun-2010. [Online]. Available: https://open.library.ubc.ca/collections/undergraduateresearch/51869 /items/1.0107224. [Accessed: 09-Oct-2019].

[14] NACA 0015 (naca0015-il). [Online]. Available: http://airfoiltools.com/airfoil/details?airfoil=naca0015-il. [Accessed: 28-Sep-2019]